Aalto University

OPEN ACCESS

This is an electronic reprint of the original article.
This reprint may differ from the original in pagination and typographic detail.

Tiainen, Tony; Myllymäki, Teemu T.T.; Hatanpää, Timo; Tenhu, Heikki; Hietala, Sami

Polyelectrolyte stabilized nanodiamond dispersions

Published in:
Diamond and Related Materials

DOI:
10.1016/j.diamond.2019.04.019

Published: 01/05/2019

Document Version
Publisher's PDF, also known as Version of record

Published under the following license:
CC BY

Please cite the original version:
Tiainen, T., Myllymäki, T. T. T., Hatanpää, T., Tenhu, H., & Hietala, S. (2019). Polyelectrolyte stabilized nanodiamond dispersions. *Diamond and Related Materials*, *95*, 185-194. https://doi.org/10.1016/j.diamond.2019.04.019

This material is protected by copyright and other intellectual property rights, and duplication or sale of all or part of any of the repository collections is not permitted, except that material may be duplicated by you for your research use or educational purposes in electronic or print form. You must obtain permission for any other use. Electronic or print copies may not be offered, whether for sale or otherwise to anyone who is not an authorised user.

Diamond & Related Materials 95 (2019) 185–194

Contents lists available at ScienceDirect

Diamond & Related Materials

journal homepage: www.elsevier.com/locate/diamond

Polyelectrolyte stabilized nanodiamond dispersions

Tony Tiainen[a], Teemu T.T. Myllymäki[b], Timo Hatanpää[a], Heikki Tenhu[a], Sami Hietala[a,*]

[a] Department of Chemistry, University of Helsinki, P.O. Box 55, FIN-00014, HU, Finland
[b] Department of Applied Physics, Aalto University, P.O. Box 15100, FI-00076 Aalto, Finland

ARTICLE INFO

Keywords:
Nanodiamond
Colloidal stability
Polyelectrolyte complex
Zeta potential

ABSTRACT

Colloidal stability of negatively charged nanodiamonds (ND) has been realized with the help of double hydrophilic block copolymers poly(ethylene oxide)-*block*-poly(dimethylaminoethyl methacrylate)-dodecyl (PEO-*b*-PDMAEMA-C12). The polymers were synthesized through RAFT polymerization of DMAEMA with a PEO macromonomer carrying trithiocarbonate and dodecyl end-groups. The NDs and the polymers were complexed by mixing them in different ratios. In addition to the amount of polymers, the effect of the detailed structure of the polymer was of interest and thus, also polymers with different lengths of the PEO-block were synthesized, as well as a block copolymer without the dodecyl end-group. The composition of the polymer, as well as the complexation conditions were varied to find the route to stable nanoparticles. The optimized complexation method gave colloidally stable ND particles with positively charged PDMAEMA coronas. The colloids were stable at room temperature and also in saline solutions up to 0.154 M NaCl.

1. Introduction

Nanodiamonds (NDs) are an intriguing class of carbon nanomaterials with a diamond-like inner structure, rich surface chemistry and size in the submicron domain [1–7]. They have surfaced as a viable material to be used in place of and in conjunction with other carbon based nanomaterials especially in engineering [8,9] and biomedicine [10,11]. The useful properties of NDs for these applications include versatile and modifiable surface [5], electric insulation, high thermal conductivity [12], good mechanical- and chemical resistance [9], biocompatibility [13] and natural non-bleaching fluorescence [14,15]. These are a result of the diamond-like properties of the ND cores combined with the variable surface functionalities accessible by different ND production processes [16]. A number of different ways to prepare NDs are available, including so called static high pressure high temperature (HPHT), dynamic detonation methods, laser ablation, microwave plasma, chemical vapor deposition (CVD) and ultrasound cavitation [7]. Of these, the most often used are the HPHT and detonation methods.

Detonation methods are a cost effective approach for producing NDs in large scale [17]. In the most utilized detonation synthesis, two explosives having a combined oxygen balance under zero (mainly trinitrotoluene (TNT) and hexogen (RDX)) are detonated in a closed chamber yielding nanoscale sp^3 carbon soot. The soot is then collected and purified to yield the end product called detonation nanodiamond. With further processing the surfaces of the detonation NDs can be functionalized in multiple ways [5], leading to *e.g.* carboxylate- or amine functionalized diamonds. However, diamonds produced by detonation may also have very complex surface functionalities. This combined with their large surface to volume ratio leads to a tendency of NDs to bind to each other by different mechanisms forming tight core agglutinates, core aggregates, intermediate aggregates and agglutinates [18]. Aggregated NDs lose many of the attractive properties stemming from their small size and make the production of heterogeneous products or stable colloidal solutions a challenging task [2].

Studies of breaking the different aggregates of NDs have been reported by many groups [3,4,18–22]. By either grinding [18], sonicating [21,22] or annealing [20,23], a colloidal dispersion of small ND particles is achievable. However, the long term stability [24],

Abbreviations: ND, detonation nanodiamond; PEO-*b*-PDMAEMA-C12, poly(ethylene oxide)-*block*-poly(dimethylaminoethyl methacrylate)-dodecyl; RAFT, reversible addition-fragmentation chain transfer polymerization; HPHT, high pressure high temperature; CVD, chemical vapor deposition; TNT, trinitrotoluene; RDX, hexogen; CTA, chain transfer agent; PEO-CTA, poly(ethylene oxide) methyl ether 2-(dodecylthiocarbonothioylthio)-2-methylpropionate; PMMA, poly(methyl methacrylate); DMF, dimethylformamide; DMAEMA, 2-(dimethylamino)ethyl methacrylate; AIBN, azobisisobutyronitrile; GPC, gel permeation chromatography; NMR, nuclear magnetic resonance (spectroscopy); FTIR, Fourier-transform infrared (spectroscopy); TGA-EGA, thermogravimetric- and evolved gas analysis; TEM, transmission electron microscopy; DLS, dynamic light scattering; ZP, Zeta Potential; UV–vis, Ultraviolet–visible (spectroscopy); IWS, ice-water-salt bath; DTG, differential thermogravimetry; EIC, extracted-ion chromatogram

* Corresponding author.
E-mail address: sami.hietala@helsinki.fi (S. Hietala).

https://doi.org/10.1016/j.diamond.2019.04.019
Received 4 February 2019; Received in revised form 16 April 2019; Accepted 17 April 2019
Available online 18 April 2019
0925-9635/ © 2019 Published by Elsevier B.V.

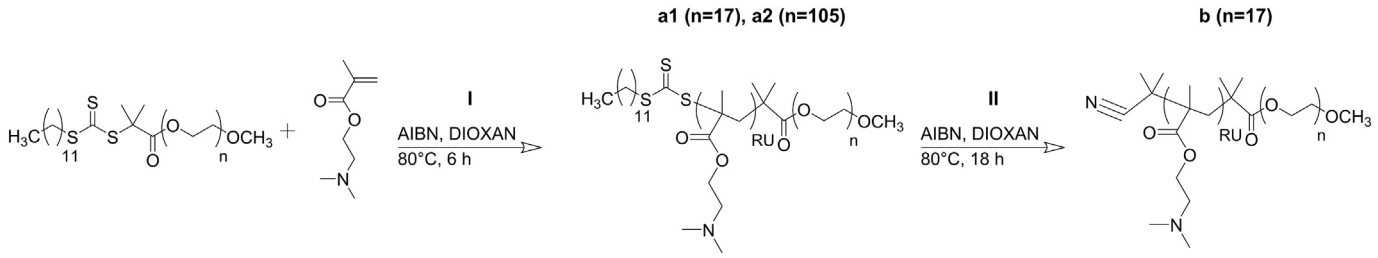

Scheme 1. RAFT polymerization (**I**) and end-group removal (**II**).

redispersibility and usability without further functionalization is difficult to achieve. To enhance these properties, methods to stabilize and functionalize NDs have been studied. Most of the approaches involve covalent functionalization of NDs with surface groups that enable longer term stability or bring additional functionality [25]. Azide-alkyne cycloaddition reactions on azide functionalized NDs have been shown to be a viable method to attach various moieties [26,27]. By attaching PEO or poly(methyl ether methacrylate) with NDs Zhang et al. demonstrated enhanced dispersibility in water [28].

The properties of NDs can also be enhanced by physical adsorption to the surface of NDs. For example doxorubicin has been complexed with negatively charged NDs in order to bind and release a drug upon varying the salt concentration [29]. Covalent and non-covalent approaches have also been combined interestingly by attaching proteins by electrostatic interactions to NDs followed by covalent protein immobilization [30]. Proteins bovine- and human serum albumin have been shown to complex fluorescent NDs and to prevent their aggregation in aqueous dispersions and be used for enhanced intracellular delivery [31]. According to the same report, block copolymers such as poly(ethylene glycol)-*block*-poly(dimethylaminoethyl methacrylate-*co*-butylmethacrylate) can also be used for this purpose. Hybrid ND:poly (ethylene imine) polyelectrolyte complexes have been utilized as vectors for siRNA delivery [32].

Polymeric dispersants can be often utilized to prevent colloid aggregation/instability. They function by adsorbing at the surface of the suspended particle and providing a protective layer that reduces particle-particle attraction and/or enhances solvent-particle interaction. PEO has been used to provide steric stabilization especially in the biomedical field [33,34]. Polyelectrolytes, on the other hand, are capable of providing electrostatic stabilization and may also enable charge inversion when oppositely charged moieties are used for complexation. PDMAEMA is a weak polycation that has been used with graphene to form colloidally stable multilayer structures sensitive to pH [35], to form pH-triggered antibiotic release systems when complexed with gelatine [36] and has also been used with carboxylated NDs to enhance their stability in biological fluids [31]. In addition, the polyelectrolyte is pH and temperature sensitive [37].

Knowing that amphiphilic PDMAEMA based block copolymers have been studied already [31], we wanted to take a step further in evaluating the effect of different structural units on the ND-polymer interaction. Multicomponent PEO-*b*-PDMAEMA-C12 polymers comprising of hydrophilic, hydrophobic and polyelectrolyte blocks are shown to enhance the stability and dispersibility of NDs in aqueous media. PEO-block lengths as well as the presence of the C12-group in the polymers were varied and their effect on the resulting polymer:ND complex properties and their colloidal stability were studied. The work demonstrates a promising approach for colloidally stable nanodiamond powder derived hybrid materials for bio- and materials applications.

2. Experimental

2.1. Materials

Carboxylated detonation nanodiamond powder with diamond content > 97%, water content ~2% and 0.07–0.1% of impurities (μDiamond® Molto Vox, Carbodeon Oy, Finland) was used as received. All solvents were used as received unless otherwise mentioned. Chain transfer agents (CTA) poly(ethylene oxide) methyl ether 2-(dodecylthiocarbonothioylthio)-2-methylpropionate (PEO17-CTA M_n 1100 g/mol and PEO105-CTA M_n 5000 g/mol, Sigma-Aldrich), poly (methyl methacrylate) (PMMA, SEC standard grade, Fluka), dimethylformamide (DMF, 99.9%, Sigma-aldrich), sodium chloride (NaCl, 99.9%, Fischer) and lithium bromide (LiBr, 99%, Fluka) were used as received. Monomer 2-(dimethylamino)ethyl methacrylate (DMAEMA, 99% stabilized, Acros organics) was run through an anhydrous alumina column (Al_2O_3, 99%, Merck) and distilled in a vacuum to remove inhibitors. Azobisisobutyronitrile (AIBN, 98%, Fluka) was recrystallized from methanol (99.9%, Sigma-Aldrich) and dissolved in 1,4-Dioxane (99%, VWR).

For preparation of aqueous solutions and dispersions, deionized ultrapure water with ~18 mΩ resistance was used. Glassware used to prepare light scattering samples and dilutions were carefully washed with methanol prior to measurement.

2.2. Synthesis of PEO-b-PDMAEMA block copolymers (I) and end-group removal (II)

The polymers were synthesized by RAFT polymerization reported earlier (Scheme 1, step I) [38]. Generally, 1 g of DMAEMA (6.35 mmol) and 46.2 mg of PEO-CTA (0.042 mmol) were weighed into a 25 mL round bottom flask followed by addition of 1 mL AIBN/dioxane solution (AIBN 0.0042 mmol/mL, 0.0042 mmol) and 4 mL of dioxane. Dissolved reagents were freeze-thawed three times under < 3 mbar vacuum to remove oxygen followed by addition of nitrogen atmosphere to the flask. The polymerization was initiated by immersing the flask into an 80 °C oil bath with magnetic stirring. The reaction was left to stir in the bath for 6 h and was stopped by placing the opened flask into an ice-water bath for 10 min.

The product was dialyzed in a MWCO 3500 g/mol cellulose membrane against deionized water for 2 days changing dialysis water at least 2 times a day. After dialysis, the product was freeze dried and stored in a freezer until used.

The removal of the dodecyl end-group was performed with a modified version of the method by Perrier et al. (Scheme 1, step II, Fig. S1–2) [39]. 0.1 g of polymer a1 (end-groups 0.0016 g, 0.00624 mmol) and 0.0154 g of AIBN (0.0936 mmol) were weighed into a 25 mL round bottom flask. The flask was sealed and purged with Ar gas for 5 min under stirring. 5 mL of dried dioxane was added through a rubber septum and the mixture was left to stir with Ar bubbling for 35 min at room temperature. The reaction was started by immersing the flask into an 80 °C oil bath with magnetic stirring. The flask was left to stir in the bath for 18 h and the reaction was stopped by placing the opened flask into an ice-water bath for 10 min. The product was purified by precipitation to cold *n*-hexane three times and dried in a vacuum. After purification, the dried product was dissolved in dioxane, freeze dried and stored in a freezer until used.

2.3. Preparation of ND dispersions and polymer solutions

A Hielscher UP400S Ultrasonic Processor was used to disperse NDs and polymer:ND complexes using a H3 sonotrode at 400 W and a 0.5 duty cycle unless otherwise mentioned. The samples were placed into an ice-water-salt bath (IWS, ~0 °C) during sonication to prevent heating of the solutions.

Stock dispersions of ND were prepared by weighing the as-received ND powder into a 20 mL glass vial, adding deionized water, mixing by hand vigorously and sonicated for 30 min. All samples were refrigerated at +4 °C when not used and sonicated at full duty cycle for 10 min prior use. The polymer solutions in water were made by dissolving polymer thoroughly into deionized water to 1 mg/mL concentrations and kept at +4 °C prior use.

2.4. Polymer:ND complexation

For the complexation experiments, a Watson-Marlow solvent pump was employed to obtain a constant addition rate of polymer solvent (0.64 mL/min). Purification and fractionation of the complexes was performed with Sigma 2K15C centrifuge at 5000 RPM (3773*g*) at 20 °C.

For the optimized procedure (see Supplementary data, Optimization of the complexation), 5 mL of refrigerated 10 mg/mL ND dispersion was measured into a 25 mL round-bottom flask with a large magnetic stirrer. The dispersion was sonicated in an IWS bath for 10 min at full duty cycle. Sonicated dispersion was moved into another IWS bath with magnetic stirring at 750 RPM. 15 mL of refrigerated 1 mg/mL polymer solution was added to the ND dispersion dropwise with a solvent pump. The mixture was left to stir for 24 h without replacing the IWS bath. After stirring, the dispersion was subjected to 120 min of sonication. For IR and TGA analysis, the complex was washed twice by centrifuging for 30 min, removing supernatant fraction and dispersing in fresh deionized water. Washed complex was dried in a 50 °C oven and stored in a desiccator if not used.

2.5. Gel permeation chromatography (GPC)

The molar masses of the polymers were determined with a Waters Acquity APC - system equipped with Acquity APC XT 200 Å, 450 Å columns and UV- and RI-detectors. DMF + 1 mg/mL LiBr was used as an eluent and molar masses were compared to PMMA standards. Samples were prepared by measuring 2 mg of sample into 1 mL of eluent and letting the sample dissolve overnight on a shaking table at room temperature. Dissolved samples were filtered through 0.45 μm PTFE filters before measurement.

2.6. Nuclear magnetic resonance (NMR)

NMR-spectra were recorded with a Bruker Avance III spectrometer operating at 500 MHz for protons. For liquid state ^{1}H measurements, the samples were dissolved in deuterium oxide (D_2O) to a concentration of 2 mg/mL. In the titration experiments a polymer sample in D_2O (2 mg/mL) was titrated by ND dispersion in D_2O (10 mg/mL), stirred and left to stabilize overnight. Stabilized sample was shaken by hand and sonicated in a bath for 30 min before measuring. Integrated solvent signal at 4.79 ppm was compared to signals at 3.71 ppm, 2.34 ppm and 1.32 ppm (Supplementary data, Fig. S1). The results were corrected to sample dilution.

2.7. Fourier-transform infrared (FTIR)

IR-spectra were collected with PerkinElmer Spectrum One using an attenuated total reflection (ATR) setup for polymers and transmission setup for ND- and complex samples. ND- and complex samples were prepared into a pellet by adding ~5–10 wt% of sample to dried KBr, mixing with a mortar and pestle to a fine powder and pressed with 10 tons of pressure for 5 min. 4 scans were taken with a range of 450–4000 cm^{-1}.

2.8. Thermogravimetric- and evolved gas analysis (TGA-EGA)

TGA-EGA analysis was done using a Netzsch STA 449 F3 Jupiter simultaneous thermal analyzer connected to JAS-Agilent GC–MS (7890B/MSD5977A). 8–10 mg of sample was weighed into an Al_2O_3 TG crucible and stabilized in the instrument at 40 °C until there was no significant mass change. In the dynamic measurements done, the sample was heated from 40 to 1200 °C with a heating rate of 5 °C/min under a 40 mL/min helium flow. Half of the gas flow containing the evolved gases was led through a heated transfer line to JAS valve box, from where the flow was continuously sampled through a 60 cm long inert GC capillary acting as a pressure restriction to the MS detector (MSD5977A).

2.9. Transmission electron microscopy (TEM)

Transmission electron microscopy was conducted to complement the size data and visualize NDs and complexes. TEM images were taken with a Jeol JEM-2800. Samples with 0.1 mg/mL concentration in water were sonicated in a water bath for 90 min, blotted on an ultrathin CF300H-Cu-UL carbon support grid and dried at ambient atmosphere.

2.10. Dynamic light scattering (DLS) and Zeta Potential (ZP)

DLS and ZP measurements were made at 25 °C with Malvern Zetasizer Nano DS instrument using a HeNe laser operating at 633 nm in a backscattering configuration. Samples were degassed and then prepared into folded capillary zeta cells with a concentration of 0.1 mg/mL. ND and complex samples were prepared without filtering to prevent adsorption of samples into filters. Each sample was measured 5 times using the average of at least 3 measurements as the result. Measurements where the quality was low or cumulant- and distribution fit errors were too high, according to Zetasizer software, were not used. To give a full view on the particle size distributions, both number and intensity weighed distributions are presented and particle sizes are given as number mean values or Z-average values from 2nd order (cumulant) polynomial fit. Smoluchowski model was used in analysis of the electrophoretic mobility and zeta potential. Stability of the dispersions was measured from the samples stored in zeta cells at different periods of time.

2.11. pH

pH was measured to determine if the basic polymer (pKa ≈ 7.5) [40] and acidic carboxylic acid (pKa ≈ 4–5) [41] on the ND surface neutralize each other during complexation. pH of the solutions and dispersions (concentration 1–10 mg/mL in deionized water) were measured at room temperature with a VWR Phenomenal IS2100L using WTW or WVR electrodes calibrated within a day of the measurement with pH 4, 7 and 10 buffers.

2.12. Stability studies

DLS and ZP samples in deionized water were stored in the folded capillary zeta cells at room temperature in the dark and measured between set time intervals up to 5 weeks of storage. For measurements under saline conditions, samples in deionized water were added to salt solutions to desired ionic strength ([NaCl] = 0.01–0.154 mol/L) and solid content of 0.1 mg/mL. Each sample in saline was measured separately within 2 h of preparation.

Table 1
Specific data of block copolymers.

Product	PEO17-*b*-PDMAEMA-C12	PEO105-*b*-PDMAEMA-C12	PEO17-*b*-PDMAEMA
Label	a1	a2	b
M:CTA:Init	150:1:0.1	200:1:0.33	1:0:16
Reaction time (h)	6	6	18
Conversion (%)	54.5	55	52.8
M_n (g/mol)			
Theoretical	13,834	22,293	15790[a]
NMR[b]	17,000	22,300	16790[a]
GPC	16,000 DMF, 17,000 THF	15,000 DMF	15790[a]
PDI	1.9 DMF, 1.3 THF	1.6 DMF	1.9
Repeating units (RU)	101	110	101
pH	8.6	9.1	8.6

[a] Molar mass was estimated assuming complete replacement of the C12-chains with butyronitrile.
[b] Molar masses (M_n) were assessed from ^{1}H NMR by comparing the PEO-block signals at 3.7 ppm to PDMAEMA side-chain CH_2-signals at 4.15 ppm (Fig. S1).

3. Results and discussion

The PEO-b-PDMAEMA-C12 polymers were synthesized *via* RAFT polymerization and subsequent post-modification (Table 1). The three polymers were synthesized to have the same PDMAEMA-block lengths, while the PEO-block length and presence of the hydrophobic C12 dodecyl end-group were varied. In order to investigate the interactions between NDs and polymers, the complexation process and the resulting complexes were first studied. Then complexation variables such as temperature, polymer to ND ratio and use of sonication were varied and their effect on the size distribution, pH and zeta potential of the complexes were monitored. Full details of the complex preparation are given in the Supplementary Data. Complexes with 20:1 (polymer:ND) molar ratio were chosen for further studies. These were then investigated to assess their size, surface charge and colloidal stability. For clarity, the polymers are labelled **a1** (PEO17-*b*-PDMAEMA-C12), **a2** (PEO105-*b*-PDMAEMA-C12) and **b** (PEO17-*b*-PDMAEMA) (Table 1) and the corresponding complexes as **C-a1**, **C-a2** and **C-b** (Table 2).

3.1. Complexation of polymers and NDs

The polymer:ND complexation was studied by ^{1}H NMR by adding ND dispersion to the polymer solution (Fig. S1). As the surface of NDs comprise mostly of carboxylic acids, especially the positively charged PDMAEMA-blocks are expected to interact with their surface. This would lead to lowered mobility of the polymer segments and consequently to suppressed NMR signal intensity. However, as the ND surfaces contain also other functional moieties capable of interacting with PEO or C12, their signals were monitored as well. The titration of polymers a1 and a2 by ND dispersion (Fig. 1) shows a decrease of signal intensities with increasing amount of ND added. By observing the change in signal intensities of block copolymer a1 (Fig. 1A), it can be concluded that all parts of the polymer lose mobility with the addition of NDs. When polymer a2 with longer PEO is studied (Fig. 1B) the PDMAEMA signal decreases similarly as with polymer a1, but the PEO and C12 signals are less suppressed compared to PDMAEMA. This shows that the electrostatic interaction between the ND carboxyls and PDMAEMA plays the main role in the complexation process. The less suppressed signal of PEO of a2 compared to a1 indicates that longer PEO-chains of a2 extend as dangling chains from the ND surface towards the solvent retaining their mobility. The situation is different for a1, where the short PEOs are embedded in the fuzzy interface. Analysis of the C12 signals in the case of a1 indicates that the dodecyl end-group is in very restricted environment due to the presence of hydrophobic interactions with the ND surface. For polymer a2, the signal from C12 suppresses less during titration, which can be related to the overall more hydrophilic nature of the a2 polymer due to the longer PEO-blocks.

IR spectrum of the NDs (Fig. 2) reveals signals corresponding to OH-groups of absorbed water, (confirmed by measuring the sample again after heating at 130 °C, Fig. S3), carboxyls and anhydrides [4,42]. The spectrum of the block copolymer is characteristic for PDMAEMA without obvious signals from PEO or dodecyl end-groups. For the purified and dried polymer:ND complex (C-a1) the signals of both polymer and ND are present. Complexes C-a2 and C-b show similar spectra as C-a1 (Fig. S4). Compared with the starting materials, the absorbances are shifted slightly indicating the binding of polymers onto the ND surfaces. Most clear indication of the interaction is the attenuation of the N-$(CH_3)_2$ signal at 2750 cm^{-1}, where the absorption band is nearly undetectable in the complex sample, as has been observed earlier for complexed PDMAEMA [43,44].

Thermal stability of NDs, polymer and complex were studied with TGA under He-atmosphere (Fig. 3). ND shows onset of degradation at 475 °C and starting from this temperature up to 900 °C. MS for the evolved gases shows a strong signal at m/z 44, assigned to CO_2 which may be assumed to form from degradation of carboxyl groups [45,46]. NDs retain 70% of their mass even when heated up to 1200 °C but change their colour to dark black which can be related to high content of sp^2 carbon [47]. Polymer a1 shows a two-step degradation pattern starting at 155 °C. Evolved gas analysis of the polymer below 300 °C indicates nearly pure evaporation of DMAEMA until further heating leads to complex pyrolysis products and oxidized carbon.

The complex C-a1 shows a combination of the degradation patterns of pure ND and polymer with three distinguishable steps. Nearly all polymer degrades prior to the onset of ND degradation, enabling the estimation of the amount of polymer in the complex. The polymer mass of the purified complex according to TGA is around 20 wt%, which corresponds well to the mass ratio of the polymer in the feed (in this complex 23.2 wt%, Table S1). Thermal analysis data of complexes containing differential thermogravimetry curve (DTG) and extracted-ion chromatograms (EIC) can be found at Supplementary data (Fig. S5).

All in all, the IR, NMR and TGA data confirm successful complexation and that the purification does not selectively wash away either of the components.

Table 2
DLS, ZP and pH data of ND and complexes.

Label	Polymer	pH[a]	Zeta potential (mV)	Size (d·nm)	PDI
C-a1	PEO17-*b*-PDMAEMA-C12	7.3	51.1	154.2[b], 27.8[c]	0.224
C-a2	PEO105-*b*-PDMAEMA-C12	7.4	44.3	190.6[b], 50.0[c]	0.310
C-b	PEO17-*b*-PDMAEMA	7.5	40.4	155.5[b], 79.7[c]	0.225
ND	–	3.8	−74.1	149.5[b], 30.5[c]	0.240

[a] pH of polymer solutions in Table 1.
[b] Z-average size (Fig. S7).
[c] Number mean size.

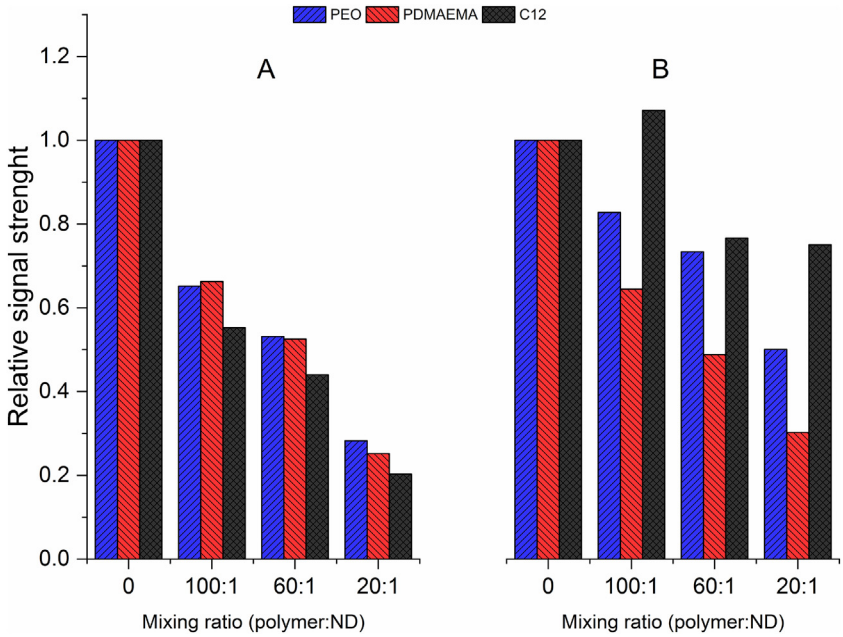

Fig. 1. ^{1}H NMR signal suppression from titration of polymers a1 (A) and a2 (B) with ND-D2O dispersion. Signal intensities of different polymer blocks are normalized with respect to dilution.

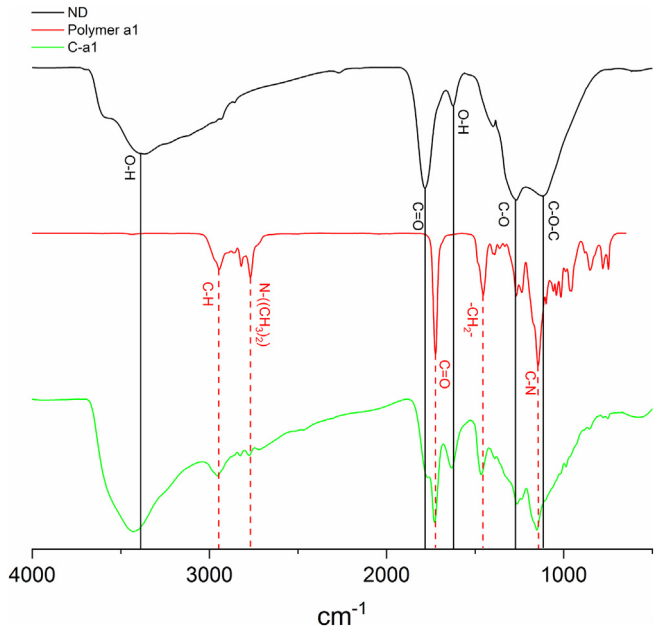

Fig. 2. FTIR-spectra of as received ND, polymer a1 and complex C-a1.

3.2. Complex characterization

When the as-received NDs are dispersed in water with stirring only, the particles remain as large aggregates and agglutinates. Sonication leads to narrower size distribution and decreased size (Fig. S6D). However, the dispersions sediment quickly due to re-formation of the larger structures. To minimize the complex size, achieve a neutral pH and maximize the surface charge of complexes for stability, the mixing ratios (polymer:ND), complexation temperatures and sonication times were varied (see Supplementary data for details, Optimization of the complexation). Generally, increasing the mixing ratio increases the size of the particles as well as their zeta potential. Initially negatively charged particles show positive zeta potential when enough polymer is added but aggregate when zeta potential is close to zero. Lowering the complexation temperature to 0 °C from room temperature results in smaller complexes and increases the zeta potential to positive value at lower mixing ratios. Even at lowest mixing ratio studied (3:1) the pH is slightly basic compared to acidic ND dispersions. Sonication up to 120 min decreased the size of the complexes considerably.

The best conditions were chosen based on the smallest size, suitable final pH value and highest surface charge obtained. Complexes with a molar mixing ratio of 20:1 (polymer:ND), mixing temperature of 0 °C and 120 min of sonication were chosen for further studies.

According to DLS the smallest complexes by number weighing are obtained by using polymer a1 with short PEO-block and C12-group (Table 2, Fig. 4A, for particle size distributions obtained by intensity weighing see Fig. S7) showing similar particle size as the pure ND dispersion after sonication. The particle size then increases for complexes with polymer a2 with longer PEO-block, which is in line with the results from NMR experiments that suggest that dangling PEO-chains may extend towards the solvent from the complexes, increasing the observed hydrodynamic diameter. Complexes obtained from the polymer without the hydrophobic C12-group, C-b, show the largest size analysed by number weighing, which is also demonstrated in a morphological change in the TEM images discussed later. The importance of hydrophobic-hydrophilic balance has also been shown for dispersing carbon nanofibers by amphiphilic PDMAEMA copolymers [48] and for fullerene C60 with alkyne-functionalized poly(oxazoline)s [49]. In both cases polymers with hydrophobic moieties were better dispersants for these carbon materials leading to smaller sized aggregates.

Upon complexation, the acidic NDs and basic polymers neutralize each other leading to changes of pH compared to the original solutions (Fig. 4B). Acidic pH < 7 indicates free ND and basic pH > 8 (Table 1) indicates free, uncomplexed polymer. Average pH of the 20:1 complexes after sonication is around 7.4. Complexes C-a1 and C-a2 have a pH of 7.6 without sonication, a 2.5% difference to the sonicated solutions which can be regarded as measurement error. For these polymers, efficient complexation between ND and polymer without large mechanical stress applied to the solution takes place. As complexes C-a1 and C-a2 have different length PEOs, we can conclude that the length of PEO-block does not significantly change the binding between the polymer and ND. However, dispersion of complex C-b without the hydrophobic C12 has a pH of 8.5 before sonication. After sonication the

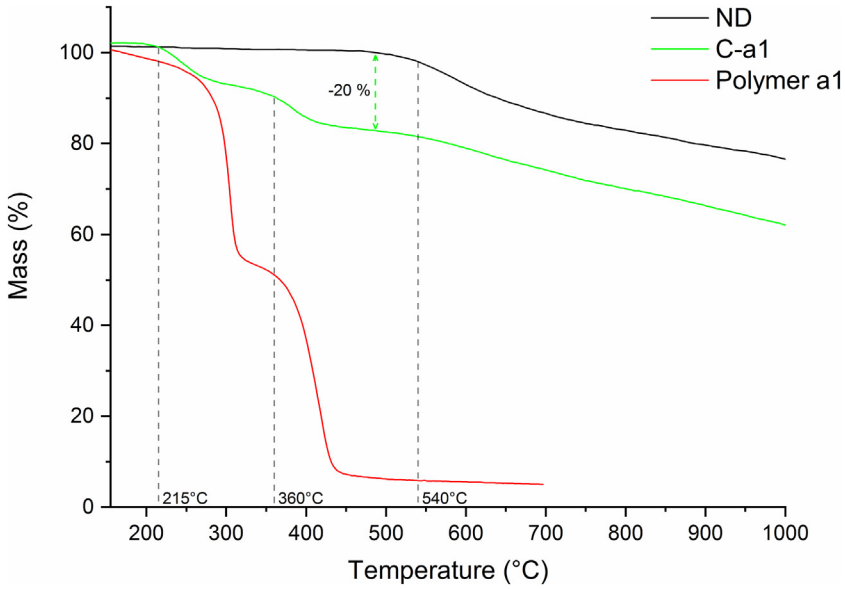

Fig. 3. TG-curves of ND, Polymer a1 and complex C-a1.

pH drops to 7.5. This shows that the binding of polymers to the ND surface is aided by the hydrophobic dodecyl end-group, which anchors the polymers to the hydrophobic sites on the NDs. After sonication the average pH of all of the 20:1 complexes is ~7.4 which is a preferable pH for many applications.

All studied complexes have a ZP above +30 mV (Fig. 4C), in contrast to the pure ND dispersion having a ZP below −60 mV. The complexation thus induces a charge inversion of the particles. For all the dispersions sonication increases the ZP if the value is positive and decreases ZP if the value is negative. This is due to the breaking down of

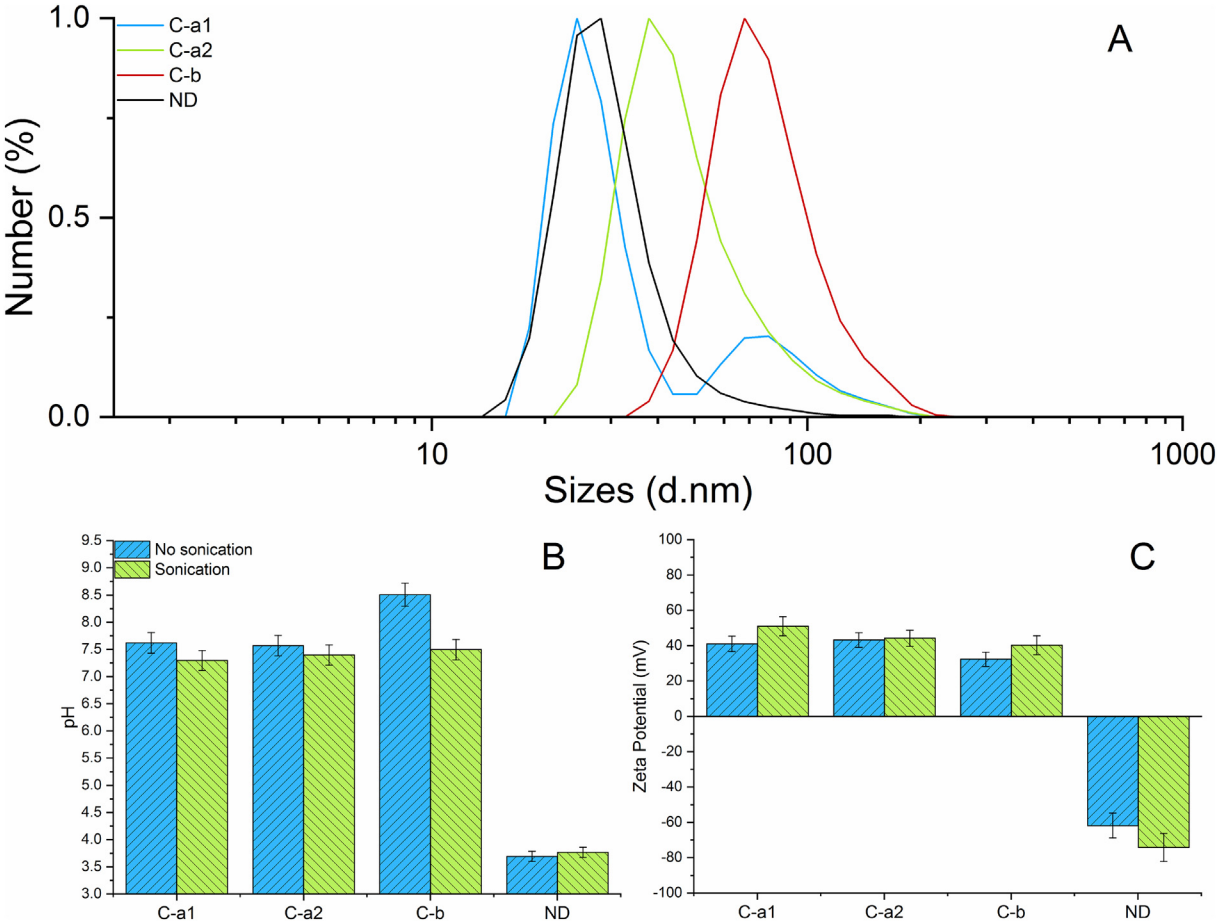

Fig. 4. Size distributions of complexes and ND by number (A) with pH- (B) and zeta potential (C) values of complexes and NDs before and after sonication. Error bars represent instrument maximum error (5%) in pH data and measured deviation in ZP data.

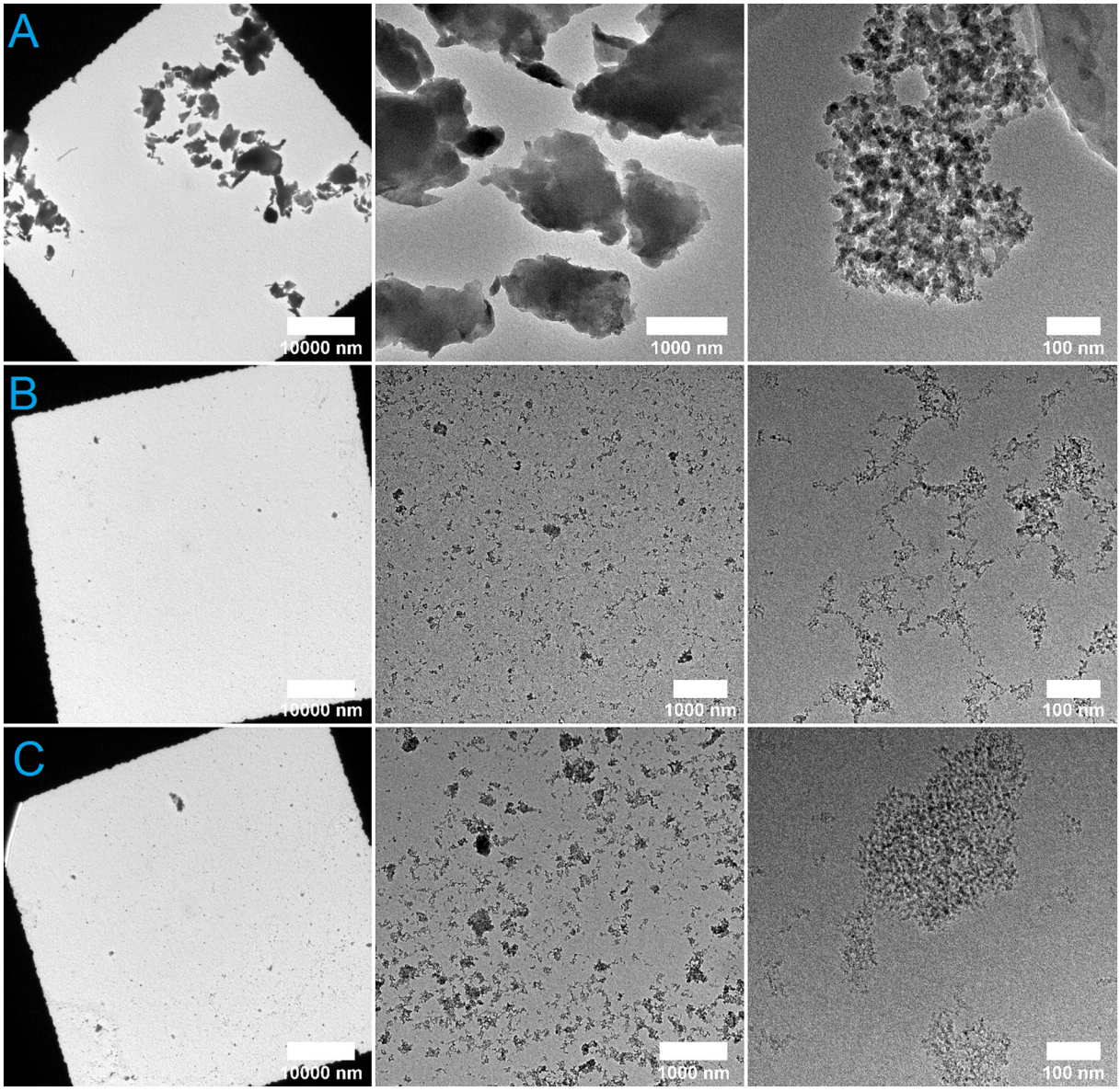

Fig. 5. TEM images of ND (A), C-a1 (B) and C-b (C). Note the increase in magnification from left to right 10,000 nm → 1000 nm → 100 nm.

the aggregates thus increasing the electrophoretic mobility of the particles being measured. The surface zeta potential > +40 mV of the sonicated complexes provides efficient electrostatic stabilization to the dispersed particles.

TEM imaging was used to visualize the NDs and their complexes (Fig. 5). The TEM images confirm large and dense aggregates for the pure ND samples, while the polymer:ND complexes are more finely and evenly dispersed at all magnifications. The complex C-a1 with the C12-chain has smaller size and is clearly more dispersed than the complex C-b. This is in line with the DLS and zeta potential measurements for C-a1 and C-b highlighting the important role of the dodecyl end-group in the complexation process.

3.3. Colloidal stability

Stability of the ND and complex dispersions in deionized water was followed using samples stored at room temperature (Fig. 6). The pure ND dispersion aggregated considerably after 1 week of storage. The average diameter nearly doubled (Fig. 6A) and the ZP halved (Fig. 6B) on top of visual observation of sedimentation. The change in ZP can be explained through the size change. As the size increases, mobility decreases and surface to volume decreases causing smaller ZPs even though there is no chemical change in the charged groups. The polymer:ND complex samples showed a small increase in size and no significant changes in ZP over 5 weeks of observation time, apart from a small fraction of sediment seen by eye. This shows clearly how complexing NDs enhance the stability of the formed dispersion significantly and the composition of polymer has little to no effect on it.

Stability of NDs and complexes C-a1 and C-a2 in saline were measured up to isotonic concentrations. Samples prepared in different NaCl solutions were measured by DLS (Fig. 7A) and ZP (Fig. 7B) within 2 h of preparation. The ND dispersion showed increased size and greatly decreased ZP immediately when salt was present. The dispersion began to precipitate already at a concentration of 0.05 mol/L and was unmeasurable by DLS at higher salt concentrations due to complete sedimentation. Complexes C-a1 and C-a2 remained in solution upon increasing ionic strength. The size of C-a1 complexes increased when the salt concentration was above 0.05 mol/L. Complexes of C-a2 retained their size relatively unchanged over the whole concentration range studied, indicating that the increased length of the PEO-block improves

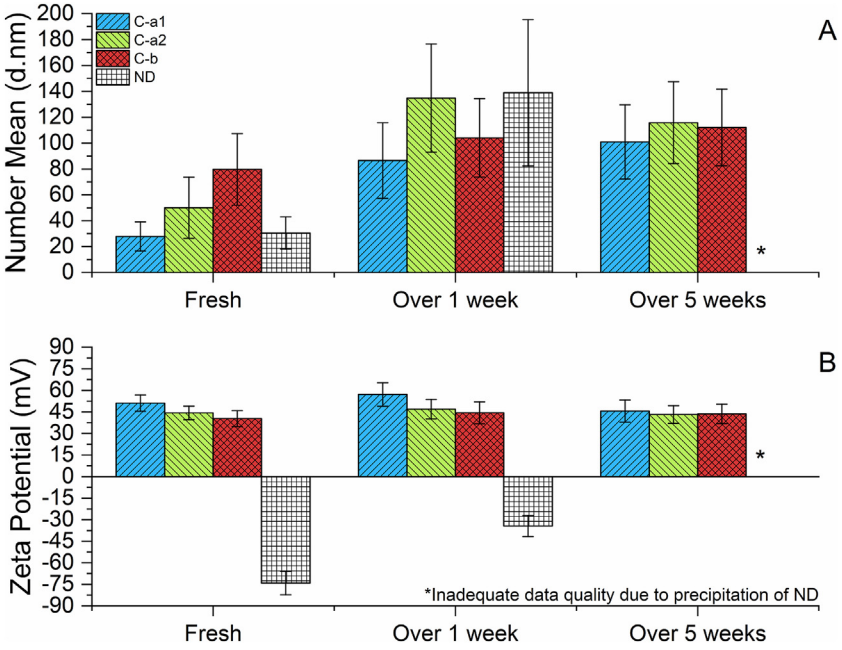

Fig. 6. Stability measurements conducted over the time span of 5 weeks. Size (A) and ZP (B) with standard deviation.

the stability. ZP of both complexes decreased due to the screening of charges. The results show that the steric stabilization provided by PEO-chains promotes the colloidal stability even though the charges are screened through increased ionic strength. Stability data according to Z-Average size is shown in Supplementary data (Fig. S8).

In addition to the described benefits by complexation of NDs for use as dispersions, in some cases it would be preferable to store and use NDs as dry powder. However, dry ND powder is difficult to handle as it whirls easily as airborne small particulates and deposits on surfaces. Dried polymer:ND complexes yield redispersable (Fig. S9), non-powdery flakes that are easier and safer to work with.

4. Conclusions

Colloidally stable dispersions of negatively charged nanodiamonds (ND) were made with amphiphilic, cationic block copolymers. Combined with sonication, polymer:ND dispersions with large positive zeta potential, neutral pH, improved colloidal stability and particle sizes below 200 nm were obtained. Complexes prepared with block copolymers having different PEO-block lengths and/or with a hydrophobic C12-group resulted in differently sized aggregates with different morphology. More finely dispersed complexes were obtained with polymers bearing the C12-group, indicating the importance of hydrophobic interactions between the ND surface and polymers. The complex

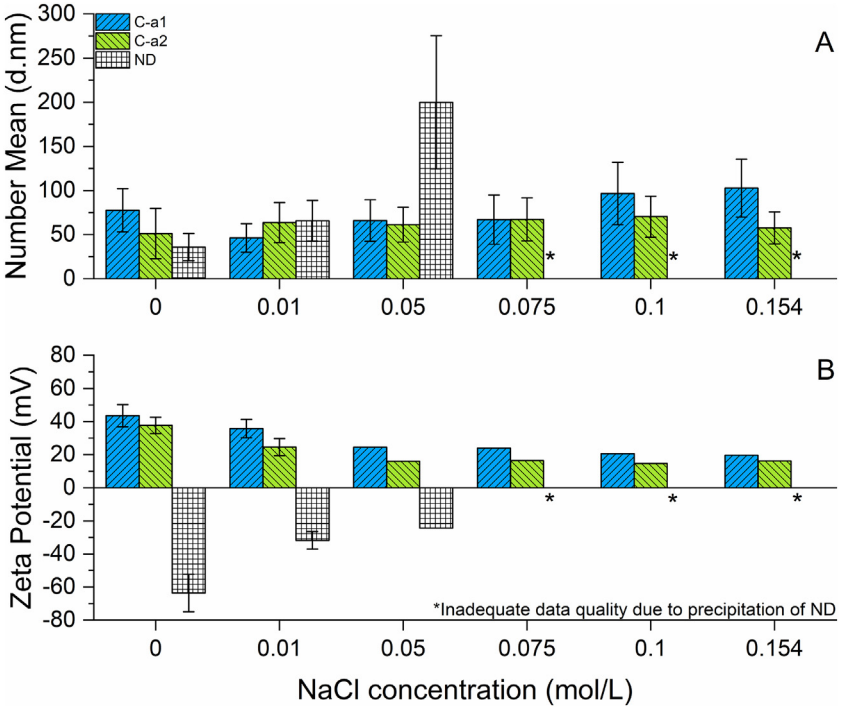

Fig. 7. Stability measurements in increasing NaCl concentration. Size with (A) and ZP (B) with standard deviation.

dispersions retain their size and colloidal stability in water for extended periods of time. Their stability was also demonstrated in saline and found to be superior compared with pure ND dispersions that aggregate and sediment. Steric stabilization provided by the longer PEO-blocks further increased the colloidal stability of the dispersions against saline. Polyelectrolyte complexation of NDs thus provides a viable way to prevent the aggregation and clustering of their dispersions and provides a promising platform for functional, dispersible ND particles for a variety of material and biological applications.

Acknowledgements

We acknowledge the provision of facilities and technical support by Aalto University at OtaNano - Nanomicroscopy Center (Aalto-NMC). We would also like to thank Carbodeon Oy for kindly providing the nanodiamonds.

Funding

This work was supported financially by the doctoral programme in Materials Research and Nanosciences (MATRENA).

Declaration of interest

None.

Appendix A. Supplementary material

Supplementary data available with the following content: *1.* ^{1}H NMR and UV-spectra of polymers, *2.* FTIR, *3.* DTG-MS, *4.* Optimization of complexation, *5.* DLS, stability and redispersion, *6.* Estimation of the molar mass of a single ND particle with a diameter of 5 nm, *7.* Sonication time. https://doi.org/10.1016/j.diamond.2019.04.019

References

[1] V. Georgakilas, J.A. Perman, J. Tucek, R. Zboril, Broad family of carbon nanoallotropes: classification, chemistry, and applications of fullerenes, carbon dots, nanotubes, graphene, nanodiamonds, and combined superstructures, Chem. Rev. 115 (2015) 4744–4822, https://doi.org/10.1021/cr500304f.
[2] A. Krueger, The structure and reactivity of nanoscale diamond, J. Mater. Chem. 18 (2008) 1485–1492, https://doi.org/10.1039/b716673g.
[3] A. Krueger, Carbon Materials and Nanotechnology, Wiley-VCH Verlag GmbH, 2010.
[4] A. Vul, O. Shenderova, Detonation Nanodiamonds: Science and Applications, Taylor & Francis, 2014.
[5] A. Krueger, D. Lang, Functionality is key: recent progress in the surface modification of nanodiamond, Adv. Funct. Mater. 22 (2012) 890–906, https://doi.org/10.1002/adfm.201102670.
[6] V.N. Mochalin, O. Shenderova, D. Ho, Y. Gogotsi, The properties and applications of nanodiamonds, Nat. Nanotechnol. 7 (2012) 11–23, https://doi.org/10.1038/nnano.2011.209.
[7] O. Shenderova, D. Gruen, Ultrananocrystalline Diamond: Synthesis, Properties and Applications, Second edition, Elsevier Inc., 2012.
[8] Y. Zhang, K.Y. Rhee, D. Hui, S.J. Park, A critical review of nanodiamond based nanocomposites: synthesis, properties and applications, Compos. Part B Eng. 143 (2018) 19–27, https://doi.org/10.1016/j.compositesb.2018.01.028.
[9] V.N. Mochalin, Y. Gogotsi, Nanodiamond-polymer composites, Diam. Relat. Mater. 58 (2015) 161–171, https://doi.org/10.1016/j.diamond.2015.07.003.
[10] K. Turcheniuk, V.N. Mochalin, Biomedical applications of nanodiamond (review), Nanotechnology 28 (2017) 1–28, https://doi.org/10.1088/1361-6528/aa6ae4.
[11] O.A. Shenderova, G.E. McGuire, Science and engineering of nanodiamond particle surfaces for biological applications (review), Biointerphases 10 (2015), https://doi.org/10.1116/1.4927679 (030802-1–23).
[12] J.J. Taha-Tijerina, T.N. Narayanan, C.S. Tiwary, K. Lozano, M. Chipara, P.M. Ajayan, Nanodiamond-based thermal fluids, ACS Appl. Mater. Interfaces 6 (2014) 4778–4785, https://doi.org/10.1021/am405575t.
[13] V. Paget, J.A. Sergent, R. Grall, S. Altmeyer-Morel, H.A. Girard, T. Petit, C. Gesset, M. Mermoux, P. Bergonzo, J.C. Arnault, S. Chevillard, Carboxylated nanodiamonds are neither cytotoxic nor genotoxic on liver, kidney, intestine and lung human cell lines, Nanotoxicology 8 (2014) 46–56, https://doi.org/10.3109/17435390.2013.855828.
[14] P. Reineck, M. Capelli, D.W.M. Lau, J. Jeske, M.R. Field, T. Ohshima, A.D. Greentree, B.C. Gibson, Bright and photostable nitrogen-vacancy fluorescence from unprocessed detonation nanodiamond, Nanoscale 9 (2017) 497–502, https://doi.org/10.1039/C6NR07834F.
[15] S. Yu, M. Kang, H. Chang, K. Chen, Y. Yu, Bright fluorescent nanodiamonds : no photobleaching and low cytotoxicity, J. Am. Chem. Soc. 127 (2005) 17604–17605, https://doi.org/10.1021/JA0567081.
[16] A.Y. Jee, M. Lee, Surface functionalization and physicochemical characterization of diamond nanoparticles, Curr. Appl. Phys. 9 (2009) 144–147, https://doi.org/10.1016/j.cap.2008.12.045.
[17] V.Y. Dolmatov, Detonation synthesis ultradispersed diamonds: properties and applications, Russ. Chem. Rev. 70 (2001) 607–626, https://doi.org/10.1070/RC2001v070n07ABEH000665.
[18] A. Krüger, F. Kataoka, M. Ozawa, T. Fujino, Y. Suzuki, A.E. Aleksenskii, A.Y. Vul, E. Osawa, Unusually tight aggregation in detonation nanodiamond: identification and disintegration, Carbon N. Y. 43 (2005) 1722–1730, https://doi.org/10.1016/j.carbon.2005.02.020.
[19] N. Nunn, M. Torelli, G. McGuire, O. Shenderova, Nanodiamond: a high impact nanomaterial, Curr. Opin. Solid State Mater. Sci. 21 (2017) 1–9, https://doi.org/10.1016/j.cossms.2016.06.008.
[20] A.E. Aleksenskiy, E.D. Eydelman, A.Y. Vul, Deagglomeration of detonation nanodiamonds, Nanosci. Nanotechnol. Lett. 3 (2011) 68–74, https://doi.org/10.1016/B978-1-4377-3465-2.00006-2.
[21] A. Pentecost, S. Gour, V. Mochalin, I. Knoke, Y. Gogotsi, Deaggregation of nanodiamond powders using salt- and sugar-assisted milling, ACS Appl. Mater. Interfaces 2 (2010) 3289–3294, https://doi.org/10.1021/am100720n.
[22] K. Turcheniuk, C. Trecazzi, C. Deeleepojananan, V.N. Mochalin, Salt-assisted ultrasonic deaggregation of nanodiamond, ACS Appl. Mater. Interfaces 8 (2016) 25461–25468, https://doi.org/10.1021/acsami.6b08311.
[23] A.T. Dideikin, A.E. Aleksenskii, M.V. Baidakova, P.N. Brunkov, M. Brzhezinskaya, V.Y. Davydov, V.S. Levitskii, S.V. Kidalov, Y.A. Kukushkina, D.A. Kirilenko, V.V. Shnitov, A.V. Shvidchenko, B. Senkovskiy, M.S. Shestakov, A.Y. Vul, Rehybridization of carbon on facets of detonation diamond nanocrystals and forming hydrosols of individual particles, Carbon N. Y. 122 (2017) 737–745, https://doi.org/10.1016/j.carbon.2017.07.013.
[24] N. Gibson, O. Shenderova, T.J.M. Luo, S. Moseenkov, V. Bondar, A. Puzyr, K. Purtov, Z. Fitzgerald, D.W. Brenner, Colloidal stability of modified nanodiamond particles, Diam. Relat. Mater. 18 (2009) 620–626, https://doi.org/10.1016/j.diamond.2008.10.049.
[25] K.N.R. Wuest, V. Trouillet, R. Köppe, P.W. Roesky, A.S. Goldmann, M.H. Stenzel, C. Barner-Kowollik, Direct light-induced (co-)grafting of photoactive polymers to graphitic nanodiamonds, Polym. Chem. 8 (2017) 838–842, https://doi.org/10.1039/C6PY02035F.
[26] Z.C. Kennedy, C.A. Barrett, M.G. Warner, Direct functionalization of acid-terminated nanodiamond with azide: enabling access to 4-substituted-1,2,3-triazole functionalized particles, Langmuir 33 (2017) 2790–2798, https://doi.org/10.1021/acs.langmuir.6b04477.
[27] A. Barras, J. Lyskawa, S. Szunerits, P. Woisel, R. Boukherroub, Direct functionalization of nanodiamond particles using dopamine derivatives, Langmuir 27 (2011) 12451–12457, https://doi.org/10.1021/la202571d.
[28] X. Zhang, C. Fu, L. Feng, Y. Ji, L. Tao, Q. Huang, S. Li, Y. Wei, PEGylation and polyPEGylation of nanodiamond, Polym. (United Kingdom) 53 (2012) 3178–3184, https://doi.org/10.1016/j.polymer.2012.05.029.
[29] H. Huang, E. Pierstorff, E. Osawa, D. Ho, Active nanodiamond hydrogels for chemotherapeutic delivery, Nano Lett. 7 (2007) 3305–3314, https://doi.org/10.1021/nl071521o.
[30] L.C.L. Huang, H.C. Chang, Adsorption and immobilization of cytochrome c on nanodiamonds, Langmuir 20 (2004) 5879–5884, https://doi.org/10.1021/la0495736.
[31] J.W. Lee, S. Lee, S. Jang, K.Y. Han, Y. Kim, J. Hyun, S.K. Kim, Y. Lee, Preparation of non-aggregated fluorescent nanodiamonds (FNDs) by non-covalent coating with a block copolymer and proteins for enhancement of intracellular uptake, Mol. BioSyst. 9 (2013) 1004–1011, https://doi.org/10.1039/c2mb25431j.
[32] M. Chen, X.Q. Zhang, H.B. Man, R. Lam, E.K. Chow, D. Ho, Nanodiamond vectors functionalized with polyethylenimine for siRNA delivery, J. Phys. Chem. Lett. 1 (2010) 3167–3171, https://doi.org/10.1021/jz1013278.
[33] A.S. Karakoti, S. Das, S. Thevuthasan, S. Seal, PEGylated inorganic nanoparticles, Angew. Chem. Int. Ed. 50 (2011) 1980–1994, https://doi.org/10.1002/anie.201002969.
[34] D. Wang, Y. Tong, Y. Li, Z. Tian, R. Cao, B. Yang, PEGylated nanodiamond for chemotherapeutic drug delivery, Diam. Relat. Mater. 36 (2013) 26–34, https://doi.org/10.1016/j.diamond.2013.04.002.
[35] J. Liu, L. Tao, W. Yang, D. Li, C. Boyer, R. Wuhrer, F. Braet, T.P. Davis, Synthesis, characterization, and multilayer assembly of pH sensitive graphene–polymer nanocomposites, Langmuir 26 (2010) 10068–10075, https://doi.org/10.1021/la1001978.
[36] H.W. Yang, J.K. Chen, S.W. Kuo, A.W. Lee, Degradable coronas comprising polyelectrolyte complexes of PDMAEMA and gelatin for pH-triggered antibiotic release, Polymer 55 (2014) 2678–2687, https://doi.org/10.1016/j.polymer.2014.04.014.
[37] E. Stubbs, E. Laskowski, P. Conor, D.A. Heinze, D. Karis, E.M. Glogowski, Control of pH- and temperature-responsive behavior of mPEG-b-PDMAEMA copolymers through polymer composition, J. Macromol. Sci. Part A Pure Appl. Chem. 54 (2017) 228–235, https://doi.org/10.1080/10601325.2017.1282694.
[38] P. Semenyuk, T. Tiainen, S. Hietala, H. Tenhu, V. Aseyev, V. Muronetz, Artificial chaperones based on thermoresponsive polymers recognize the unfolded state of the protein, Int. J. Biol. Macromol. 121 (2019) 536–545, https://doi.org/10.1016/j.ijbiomac.2018.10.031.
[39] S. Perrier, P. Takolpuckdee, C.A.A. Mars, Reversible addition-fragmentation chain transfer polymerization: end group modification for functionalized polymers and chain transfer agent recovery, Macromolecules 38 (2005) 2033–2036, https://doi.

org/10.1021/ma047611m.
[40] P. van de Wetering, N.J. Zuidam, M.J. van Steenbergen, O.A.G.J. van der Houwen, W.J.M. Underberg, W.E. Hennink, A mechanistic study of the hydrolytic stability of poly(2-(dimethylamino)ethyl methacrylate), Macromolecules 31 (1998) 8063–8068, https://doi.org/10.1021/ma980689g.
[41] D.R. Lide, CRC Handbook of Chemistry and Physics, 84th Edition, 2003–2004, 84th ed., CRC Press, 2003.
[42] R.M. Silverstein, F.X. Webster, D. Kiemle, Spectrometric Identification of Organic Compounds, Sevent edi, John Wiley & Sons, Inc., 2005.
[43] J.K. Park, J. Zhang, R. Roy, S. Ge, P.D. Hustad, Polyelectrolyte multilayer-like films from layer-by-layer processing of protected polyampholytic block copolymers, Chem. Commun. 54 (2018) 9478–9481, https://doi.org/10.1039/c8cc04492a.
[44] J.A. Montaña, L.D. Perez, Y. Baena, A pH-responsive drug delivery matrix from an interpolyelectrolyte complex: preparation and pharmacotechnical properties, Braz. J. Pharm. Sci. 54 (2018) 1–10, https://doi.org/10.1590/s2175-97902018000217183.
[45] V.N. Mochalin, I. Neitzel, B.J.M. Etzold, A. Peterson, G. Palmese, Y. Gogotsi, Covalent incorporation of aminated nanodiamond into an epoxy polymer network, ACS Nano 5 (2011) 7494–7502, https://doi.org/10.1021/nn2024539.
[46] H. Boehm, Surface oxides on carbon and their analysis: a critical assessment, Carbon N. Y. 40 (2002) 145–149, https://doi.org/10.1016/S0008-6223(01)00165-8.
[47] S. Osswald, G. Yushin, V. Mochalin, S.O. Kucheyev, Y. Gogotsi, Control of sp2/sp3 carbon ratio and surface chemistry of nanodiamond powders by selective oxidation in air, J. Am. Chem. Soc. 128 (2006) 11635–11642, https://doi.org/10.1021/ja063303n.
[48] Z. Yu, K. Xu, Z. Fu, X. Liu, Y. Zhang, J. Peng, M. Chen, RAFT synthesis of polyethylene glycol (PEG) and amino-functionalized amphiphilic copolymers for dispersing carbon nanofibers, RSC Adv. 5 (2015) 23683–23690, https://doi.org/10.1039/c4ra15925j.
[49] J.F.R. Van Guyse, V.R. de la Rosa, R. Lund, M. De Bruyne, R. De Rycke, S.K. Fillipov, R. Hoogenboom, Striking effect of polymer end-group on C 60 nanoparticle formation by high shear vibrational milling with alkyne-functionalized poly(2-oxazoline)s, ACS Macro Lett. 8 (2019) 172–176, https://doi.org/10.1021/acsmacrolett.8b00998.